

Free Convection Boundary-Layer Flow over a Vertical Wavy Surface Embedded in Bidisperse Porous Media

Ching-Yang Cheng

Abstract—This work studies the free convection boundary-layer flow over a vertical wavy surface in bidisperse porous media with constant wall temperature. The two-velocity two-temperature model is used to derive the nonsimilar equations. The transformed equations of the boundary layer are solved by the cubic spline collocation method. The effects of the dimensionless amplitude, the inter-phase heat transfer parameter, the modified thermal conductivity ratio, and the permeability ratio on the heat transfer and flow characteristics have been studied. Results show an increase in the modified thermal conductivity ratio or the permeability ratio tends to increase the free convection heat transfer rate of the vertical wavy surface in bidisperse porous media. As the dimensionless amplitude increases, both the fluctuations of the local Nusselt number for the f-phase and the p-phase with the streamwise coordinate are enhanced.

Index Terms—free convection, bidisperse porous medium, vertical wavy surface, boundary layer flow.

I. INTRODUCTION

THE applications of bidisperse porous media can be found in bidisperse absorbent for enhancing absorption performance, or in bidisperse capillary wicks within a heat pipe for enhancing heat pipe heat transfer rate. There are many papers on the heat transfer of free convection or mixed convection in bidisperse porous media. Nield and Kuznetsov [1] studied the conjugate forced heat transfer in bi-disperse porous medium channel. Nield and Kuznetsov [2] used a two-velocity two-temperature model to study the forced convection in a channel for a bi-disperse porous medium. Nield and Kuznetsov [3] examined the onset of convection in a bidisperse porous medium. Nield and Kuznetsov [4] studied the effect of combined vertical and horizontal heterogeneity on the onset of convection in a bidisperse porous medium. Nield and Kuznetsov [5] examined the free convection about a vertical plate embedded in a bidisperse porous medium.

Manuscript received November 19, 2013; received March 21, 2014.

This work was supported by the National Science Council of Republic of China under the grant no. NSC 101-2221-E-218-015.

Ching-Yang Cheng is with the Department of Mechanical Engineering, Southern Taiwan University of Science and Technology, Yungkuang, Tainan 71005, Taiwan (phone: +886-6-2683734; fax: +886-6-2895877; e-mail: cycheng@mail.stust.edu.tw).

Rees et al. [6] studied the vertical free convective boundary-layer flow in bidisperse porous media. Straughan [7] examined the Nield-Kuznetsov theory for convection in a bidisperse porous medium. Kumari and Pop [8] studied the mixed convection boundary layer flow over a horizontal circular cylinder embedded in a bidisperse porous medium. Grosan et al. [9] studied the free convection heat transfer in a square cavity filled with a bidisperse porous medium. Narasimhan and Reddy [10] studied the free convection inside a bidisperse porous medium enclosure. Narasimhan and Reddy [11] examined the resonance of free convection inside a bidisperse porous medium enclosure. Nield and Kuznetsov [12] studied the forced convection in a channel partly occupied in a bidisperse porous medium.

This work studies the free convection boundary-layer flow over a vertical wavy surface in bidisperse porous media with constant wall temperature. The two-velocity two-temperature formulation is used to derive the nonsimilar governing differential equations. The transformed equations of the boundary layer are solved by the cubic spline collocation method. The effects of the dimensionless amplitude, the inter-phase heat transfer parameter, the modified thermal conductivity ratio, and the permeability ratio on the free convection heat transfer characteristics are studied.

II. ANALYSIS

Consider the free convection boundary layer flow from a vertical wavy surface in bidisperse porous media, as shown in Fig.1. The wavy surface profile is given by

$$\bar{y} = \bar{\sigma}(\bar{x}) = \bar{a} \sin(\pi \bar{x} / l) \quad (1)$$

where \bar{a} is the amplitude of the wavy surface, and $2l$ is the characteristic length of the wavy surface. The surface of the wavy surface is maintained at a constant temperature T_w , which is different from the porous medium temperature sufficiently far from the surface of the wavy surface.

A bidisperse porous medium is a porous medium in which the solid phase is replaced by another porous medium. There are two phases, as shown in Fig. 2. One is the f-phase and the other is the p-phase. In a bidisperse porous medium, the fluid occupies all of the f-phase and a fraction of the p-phase. We denote the volume fraction of the f-phase by ϕ and the porosity within the p-phase by ε . Thus $1 - \phi$ is the volume

fraction of the p-phase, and the volume fraction of the bidisperse porous medium by the fluid is $\phi + (1 - \phi)\epsilon$. Here we denote T_f and T_p as the volume-averaged temperature of the f-phase and the p-phase respectively. The volume average of the temperature over the fluid is given by

$$T_F = \frac{\phi T_f + (1 - \phi)\epsilon T_p}{\phi + (1 - \phi)\epsilon} \quad (2)$$

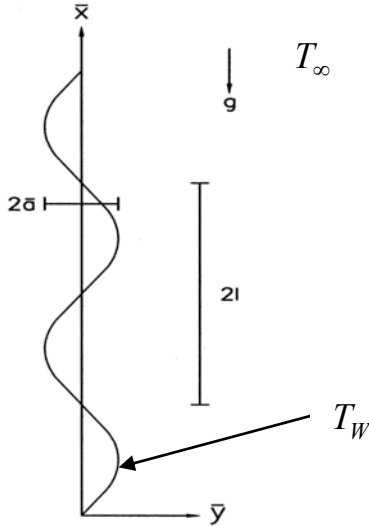


Fig. 1. Physical model and coordinates for a vertical wavy surface.

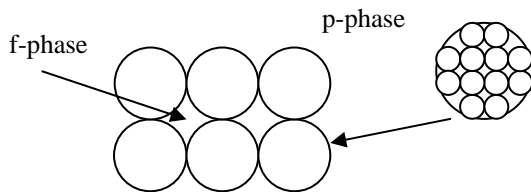


Fig. 2 Sketch of a bidisperse porous medium.

The fluid properties are assumed to be constant except for density variations in the buoyancy force term. The governing equations for the flow, heat transfer near the vertical cone can be written as [5, 13]

$$\frac{\partial \bar{u}_f}{\partial \bar{x}} + \frac{\partial \bar{v}_f}{\partial \bar{y}} = 0 \quad (3)$$

$$\frac{\partial \bar{u}_p}{\partial \bar{x}} + \frac{\partial \bar{v}_p}{\partial \bar{y}} = 0 \quad (4)$$

$$\frac{\mu}{K_f} \left(1 + \frac{\zeta K_f}{\mu} \right) \left(\frac{\partial \bar{u}_f}{\partial \bar{y}} - \frac{\partial \bar{v}_f}{\partial \bar{x}} \right) = \zeta \left(\frac{\partial \bar{u}_p}{\partial \bar{y}} - \frac{\partial \bar{v}_p}{\partial \bar{x}} \right) + \rho_F \beta_T g^* \frac{\partial T_F}{\partial \bar{y}} \quad (5)$$

$$\frac{\mu}{K_p} \left(1 + \frac{\zeta K_p}{\mu} \right) \left(\frac{\partial \bar{u}_p}{\partial \bar{y}} - \frac{\partial \bar{v}_p}{\partial \bar{x}} \right) = \zeta \left(\frac{\partial \bar{u}_f}{\partial \bar{y}} - \frac{\partial \bar{v}_f}{\partial \bar{x}} \right)$$

$$+ \rho_F \beta_T g^* \frac{\partial T_F}{\partial \bar{y}} \quad (6)$$

$$\phi(\rho c)_f \left(\bar{u}_f \frac{\partial T_f}{\partial \bar{x}} + \bar{v}_f \frac{\partial T_f}{\partial \bar{y}} \right) = \phi k_f \left(\frac{\partial^2 T_f}{\partial \bar{x}^2} + \frac{\partial^2 T_f}{\partial \bar{y}^2} \right) + h(T_p - T_f) \quad (7)$$

$$(1 - \phi)(\rho c)_p \left(\bar{u}_p \frac{\partial T_p}{\partial \bar{x}} + \bar{v}_p \frac{\partial T_p}{\partial \bar{y}} \right) = (1 - \phi)k_p \left(\frac{\partial^2 T_p}{\partial \bar{x}^2} + \frac{\partial^2 T_p}{\partial \bar{y}^2} \right) + h(T_f - T_p) \quad (8)$$

where u_f and v_f are the volume-averaged velocity components of the f-phase in the x and y directions. u_p and v_p are the volume-averaged velocity components of the p-phase in the x and y directions. K_f and K_p are the permeabilities of the two phases, and ζ is the coefficient for momentum transfer between the two phases. ρ_f is the fluid density. β_T is the volumetric thermal expansion coefficient of the fluid. μ is the viscosity of the fluid. Moreover, c is the specific heat at constant pressure and k is the thermal conductivity. Moreover, h is the inter-phase heat transfer coefficient, and g^* is the gravitational acceleration.

The boundary conditions for this problem are

$$\bar{y} = \bar{\sigma}(\bar{x}) : T_f = T_w, T_p = T_w, \bar{v}_f = 0, \bar{v}_p = 0, \quad (9)$$

$$\bar{y} \rightarrow \infty : T_f \rightarrow T_\infty, T_p \rightarrow T_\infty, \bar{u}_f \rightarrow 0, \bar{u}_p \rightarrow 0 \quad (10)$$

Here we introduce the stream functions, ψ_f and ψ_p , to satisfy the relations:

$$\bar{u}_f = \frac{\partial \bar{\psi}_f}{\partial \bar{y}}, \bar{v}_f = -\frac{\partial \bar{\psi}_f}{\partial \bar{x}}, \bar{u}_p = \frac{\partial \bar{\psi}_p}{\partial \bar{y}}, \bar{v}_p = -\frac{\partial \bar{\psi}_p}{\partial \bar{x}} \quad (11)$$

Moreover, we define the nondimensional variables and parameters:

$$x = \frac{\bar{x}}{l}, \quad y = \frac{\bar{y}}{l}, \quad a = \frac{\bar{a}}{l}, \quad \psi_f = \frac{(\rho c)_f}{\phi k_f x_0} \bar{\psi}_f, \quad \psi_p = \frac{(\rho c)_p}{(1 - \phi) k_p x_0} \bar{\psi}_p, \quad \theta_f = \frac{T_f - T_\infty}{T_w - T_\infty}, \quad \theta_p = \frac{T_p - T_\infty}{T_w - T_\infty} \quad (12)$$

Eqs. (3)-(8) become the following equations:

$$(1 + \sigma_f) \left(\frac{\partial^2 \psi_f}{\partial \bar{x}^2} + \frac{\partial^2 \psi_f}{\partial \bar{y}^2} \right) - \beta \sigma_f \left(\frac{\partial^2 \psi_p}{\partial \bar{x}^2} + \frac{\partial^2 \psi_p}{\partial \bar{y}^2} \right) = Ra \left[\tau \frac{\partial \theta_f}{\partial \bar{y}} + (1 - \tau) \frac{\partial \theta_p}{\partial \bar{y}} \right] \quad (13)$$

$$-\sigma_f \left(\frac{\partial^2 \psi_f}{\partial x^2} + \frac{\partial^2 \psi_f}{\partial y^2} \right) + \beta \left(\frac{1}{K_r} + \sigma_f \right) \left(\frac{\partial^2 \psi_p}{\partial x^2} + \frac{\partial^2 \psi_p}{\partial y^2} \right) = \tau \frac{\partial \theta_f}{\partial \tilde{y}} + (1-\tau) \frac{\partial \theta_p}{\partial \tilde{y}} \quad (22)$$

$$= Ra \left[\tau \frac{\partial \theta_f}{\partial \tilde{y}} + (1-\tau) \frac{\partial \theta_p}{\partial \tilde{y}} \right] \quad (14)$$

$$\phi \left(\frac{\partial \psi_f}{\partial y} \frac{\partial \theta_f}{\partial x} - \frac{\partial \psi_f}{\partial x} \frac{\partial \theta_f}{\partial y} \right) = \tau \frac{\partial \theta_f}{\partial \tilde{y}} + (1-\tau) \frac{\partial \theta_p}{\partial \tilde{y}} \quad (23)$$

$$= \left(\frac{\partial^2 \theta_f}{\partial x^2} + \frac{\partial^2 \theta_f}{\partial y^2} \right) + H(\theta_p - \theta_f) \quad (15)$$

$$(1+\sigma_x^2) \left[-\sigma_f \frac{\partial^2 \tilde{\psi}_f}{\partial \tilde{y}^2} + \beta \left(\frac{1}{K_r} + \sigma_f \right) \frac{\partial^2 \tilde{\psi}_p}{\partial \tilde{y}^2} \right] = \tau \frac{\partial \theta_f}{\partial \tilde{y}} + (1-\tau) \frac{\partial \theta_p}{\partial \tilde{y}} \quad (24)$$

$$(1-\phi) \left(\frac{\partial \psi_p}{\partial y} \frac{\partial \theta_p}{\partial x} - \frac{\partial \psi_p}{\partial x} \frac{\partial \theta_p}{\partial y} \right) = \phi \left(\frac{\partial \tilde{\psi}_f}{\partial \tilde{y}} \frac{\partial \theta_f}{\partial \tilde{x}} - \frac{\partial \tilde{\psi}_f}{\partial \tilde{x}} \frac{\partial \theta_f}{\partial \tilde{y}} \right) \quad (24)$$

$$= \left(\frac{\partial^2 \theta_p}{\partial x^2} + \frac{\partial^2 \theta_p}{\partial y^2} \right) + \gamma H(\theta_f - \theta_p) \quad (16)$$

$$(1+\sigma_x^2) \frac{\partial^2 \theta_p}{\partial \tilde{y}^2} - H(\theta_f - \theta_p) = \phi \left(\frac{\partial \tilde{\psi}_f}{\partial \tilde{y}} \frac{\partial \theta_f}{\partial \tilde{x}} - \frac{\partial \tilde{\psi}_f}{\partial \tilde{x}} \frac{\partial \theta_f}{\partial \tilde{y}} \right) \quad (25)$$

where the Darcy-Rayleigh number based on the characteristic length l and properties in the f-phase is given by

$$Ra = \frac{\rho_F g^* \beta_T K_f l (T_w - T_\infty)}{\mu \phi k_f / (\rho c)_f} \quad (17)$$

Moreover, the modified thermal capacity ratio, the f-phase momentum transfer parameter, the porosity parameter, permeability ratio, the modified thermal conductivity ratio, and the inter-phase heat transfer parameter are respectively defined as

$$\beta = \frac{(1-\phi)k_p(\rho c)_f}{\phi k_f(\rho c)_p}, \quad \sigma_f = \frac{\zeta K_f}{\mu}, \quad \tau = \frac{\phi}{\phi + (1-\phi)\varepsilon}, \quad (18)$$

$$K_r = \frac{K_p}{K_f}, \quad \gamma = \frac{\phi k_f}{(1-\phi)k_p}, \quad H = \frac{hl^2}{\phi k_f}$$

The associated boundary conditions are given by

$$y = \sigma(x) = a \sin(\pi x): \psi_f = 0, \psi_p = 0, \theta_f = 1, \theta_p = 1 \quad (19)$$

$$y \rightarrow \infty: \frac{\partial \psi_f}{\partial y} \rightarrow 0, \frac{\partial \psi_p}{\partial y} \rightarrow 0, \theta_f \rightarrow 0, \theta_p \rightarrow 0 \quad (20)$$

We can transfer the effect of wavy surface from the boundary conditions into the governing equations by the coordinate transformation given by

$$\tilde{x} = x, \quad \tilde{y} = Ra_l^{1/2} [y - \sigma(x)], \quad \tilde{\psi}_f = Ra_l^{-1/2} \psi_f, \quad (21)$$

$$\tilde{\psi}_p = Ra_l^{-1/2} \psi_p$$

Substituting Eq. (21) into Eqs. (13)-(16) and using boundary-layer approximation, we can obtain the following boundary-layer equations:

$$(1+\sigma_x^2) \left[(1+\sigma_f) \frac{\partial^2 \tilde{\psi}_f}{\partial \tilde{y}^2} - \beta \sigma_f \frac{\partial^2 \tilde{\psi}_p}{\partial \tilde{y}^2} \right]$$

Table 1. Comparison of values of $-\theta'_{mp}|_{\eta=0}$ for free convection heat transfer from a vertical plate with constant wall temperature in mono-disperse porous media.

$-\theta'_{mp} _{\eta=0}$		
Cheng and Minkowycz [15]	Rees and Pop [16]	Present
0.4440	0.44378	0.4442

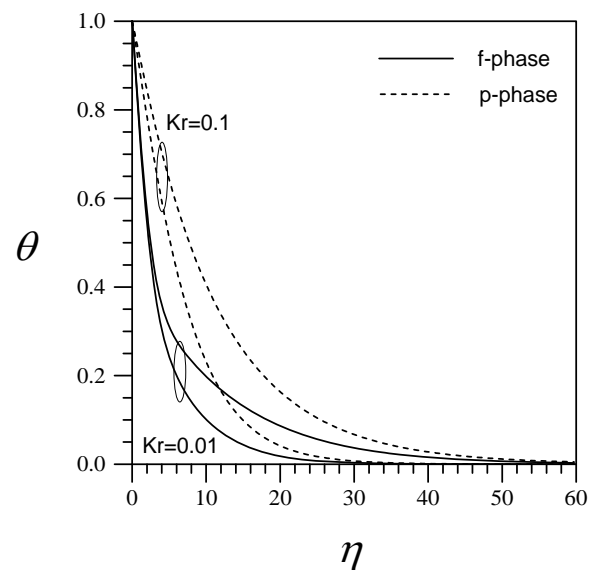


Fig. 3 The effect of the permeability ratio on the temperature profiles for the f-phase and the p-phase for $\xi = 0.3$, $H = 0.6$, $\beta = 1$, $\gamma = 0.1$, $\sigma_f = 0.01$, $\phi = 0.5$, $\varepsilon = 0.4$, and $\tau = 5/7$.

We may reduce Eqs. (22)-(25) to a form more convenient for numerical solution by the transformation:

$$\xi = \tilde{x} \quad , \quad \eta = \tilde{y} / \left[(1 + \sigma_\xi^2) \xi^{1/2} \right] \quad , \quad \tilde{\psi}_p = \xi^{1/2} g(\xi, \eta) \quad , \quad \tilde{\psi}_f = \xi^{1/2} f(\xi, \eta) \quad (26)$$

Substituting Eq. (26) into Eqs. (22)-(25), we obtain the following equations:

$$(1 + \sigma_f) f' - \beta \sigma_f g' = \tau \theta_f + (1 - \tau) \theta_p \quad (27)$$

$$-\sigma_f f' + \beta (K_r^{-1} + \sigma_f) g' = \tau \theta_f + (1 - \tau) \theta_p \quad (28)$$

$$\theta_f'' + \frac{1}{2} \phi f \theta_f' - H \xi (\theta_f - \theta_p) = \phi \xi \left(f' \frac{\partial \theta_f}{\partial \xi} - \theta_f' \frac{\partial f}{\partial \xi} \right) \quad (29)$$

$$\theta_p'' + \frac{1}{2} (1 - \phi) g \theta_p' - \gamma H \xi (\theta_p - \theta_f) = (1 - \phi) \xi \left(g' \frac{\partial \theta_p}{\partial \xi} - \theta_p' \frac{\partial g}{\partial \xi} \right) \quad (30)$$

where primes denote differentiation with respect to η . Note that the momentum equations have been integrated once about η to obtain Eqs. (27) and (28).

The boundary conditions are transformed to

$$\eta = 0: f = 0, g = 0, \theta_f = 1, \theta_p = 1 \quad (31)$$

$$\eta \rightarrow \infty: f' \rightarrow 0, g' \rightarrow 0, \theta_f \rightarrow 0, \theta_p \rightarrow 0 \quad (32)$$

Moreover, the local Nusselt numbers for the f-phase and the p-phase can be derived as

$$\frac{Nu_f}{\sqrt{Ra_{\bar{x}}}} = - \frac{\theta_f'(\xi, 0)}{(1 + \sigma_\xi^2)^{1/2}} \quad (33)$$

$$\frac{Nu_p}{\sqrt{Ra_{\bar{x}}}} = - \frac{\theta_p'(\xi, 0)}{(1 + \sigma_\xi^2)^{1/2}} \quad (34)$$

where $Nu_f = h_f \bar{x} / k_f$ and $Nu_p = h_p \bar{x} / k_p$. Note that h_f and h_p are the convection heat transfer coefficient for the f-phase and the p-phase. The Darcy-Rayleigh number based on the streamwise coordinate \bar{x} and properties in the f-phase is given by

$$Ra_x = \frac{\rho_F g^* \beta_T (T_w - T_\infty) K_f \bar{x}}{\mu \phi k_f / (\rho c)_f} \quad (35)$$

III. RESULTS AND DISCUSSION

The transformed governing partial differential equations, Eqs. (29) and (30), and the associated boundary conditions, Eqs. (31) and (32), can be solved by the cubic spline collocation method [14]. The velocities f' and g' are calculated from the momentum equations, Eqs. (27) and (28).

Moreover, the Simpson's rule for variable grids is used to calculate the values of f and g at every position from the boundary conditions, Eqs. (31) and (32). At every position, the iteration process continues until the convergence criterion for all the variables, 10^{-6} , is achieved. Variable grids with 350 grid points are used in the η -direction. The optimum value of boundary layer thickness is used. Moreover, the backward finite difference is used to calculate the derivative about the streamwise coordinate ξ .

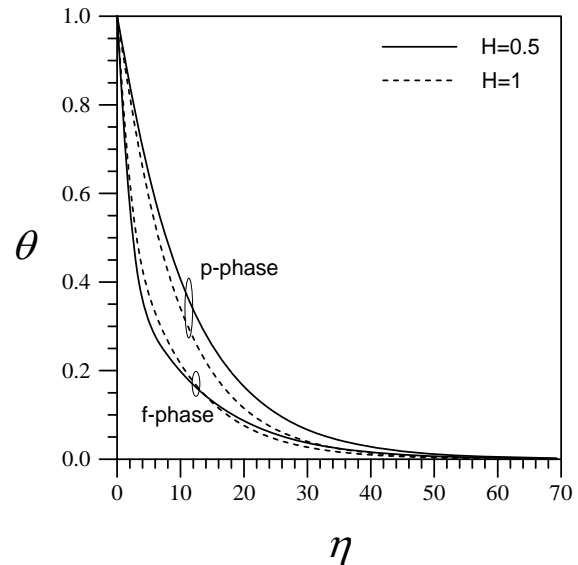


Fig. 4 The effect of the inter-phase heat transfer parameter on the temperature profiles for the f-phase and the p-phase for $\xi = 0.3$, $a = 0.2$, $K_r = 0.01$, $\beta = 1$, $\gamma = 0.1$, $\sigma_f = 0.01$, $\phi = 0.5$, $\varepsilon = 0.4$, and $\tau = 5/7$.

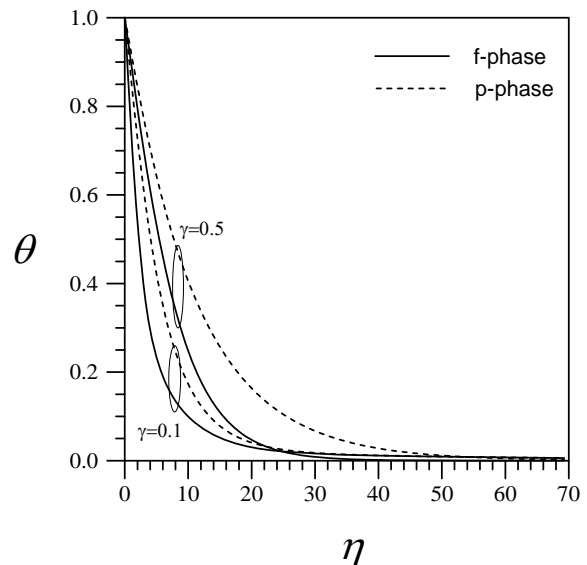


Fig. 5 The effect of the modified thermal conductivity ratio on the temperature profiles for the f-phase and the p-phase for $\xi = 0.3$, $H = 0.5$, $K_r = 0.01$, $\beta = 1$, $\sigma_f = 0.01$, $\phi = 0.5$, $\varepsilon = 0.4$, and $\tau = 5/7$.

To assess the accuracy of the solution, the present results are compared with the results obtained by other researchers. Table 1 shows the numerical values of $-\theta'_{mp} \big|_{\eta=0}$ for free convection heat transfer of a vertical

smooth plate in mono-disperse porous media with constant wall temperature. The present results are in excellent agreement with the results reported by Cheng and Minkowycz [15] and Rees and Pop [16].

Fig. 3 shows the effect of the permeability ratio Kr on the temperature profiles for the f-phase and the p-phase. As the permeability ratio is increased, both the boundary layers of the solid phase and the fluid phase become thinner, thus increasing the temperature gradients of the f-phase and the p-phase. Moreover, a decrease in the permeability ratio tends to increase the temperature difference between the f-phase and the p-phase, thus enhancing the thermal non-equilibrium effect.

Fig. 4 shows the effect of the inter-phase heat transfer parameter H on the temperature profiles for the f-phase and the p-phase. Results show that a decrease in the inter-phase heat transfer parameter tends to increase the temperature difference between the f-phase and the p-phase, thus enhancing the thermal non-equilibrium effect. In other words, when the inter-phase heat transfer parameter is small, the temperature field corresponding to the p-phase occupies a much greater region than does the temperature field of the f-phase.

Fig. 5 shows the effect of the modified thermal conductivity ratio γ on the temperature profiles for the f-phase and the p-phase. As the modified thermal conductivity ratio is increased, both the boundary layers of the solid phase and the fluid phase become thinner, thus increasing the temperature gradients of the f-phase and the p-phase. Moreover, decreasing the modified thermal conductivity ratio increases the temperature difference between the f-phase and p-phase, thus enhancing the thermal non-equilibrium effect.

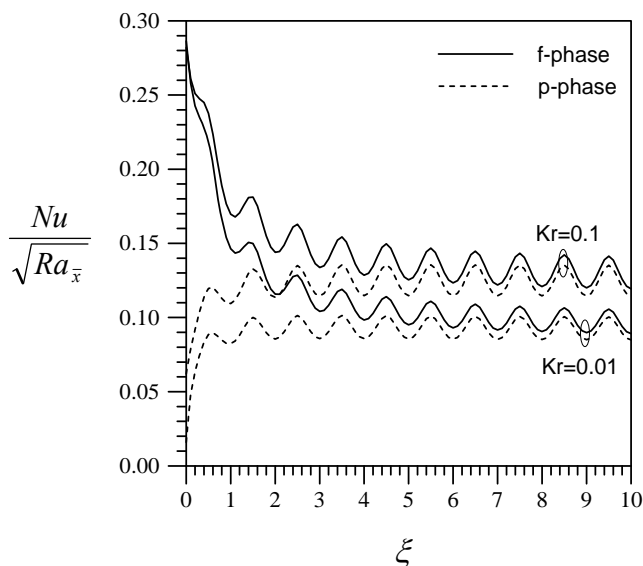


Fig. 6 The effect of the permeability ratio on the local Nusselt numbers for the f-phase and the p-phase for $a = 0.2$, $H = 0.5$, $\beta = 1$, $\gamma = 0.1$, $\sigma_f = 0.01$, $\phi = 0.5$, $\varepsilon = 0.4$, and $\tau = 5/7$.

Fig. 6 shows the effect of the permeability ratio Kr on the local Nusselt numbers for the f-phase and the p-phase. Results show that an increase in the permeability ratio tends

to increase both the local Nusselt numbers for the f-phase and the p-phase. In other words, the heat transfer rate for the bidisperse porous medium can be effectively increased by raising the permeability ratio. Moreover, with smaller coordinates, the local Nusselt number for the f-phase is much higher than that for the p-phase. The two phases are in the state of thermal non-equilibrium. As the streamwise coordinate is increased, the local Nusselt number for the f-phase approaches that for the p-phase. The bidisperse porous medium gradually approaches the state of thermal equilibrium far downstream.

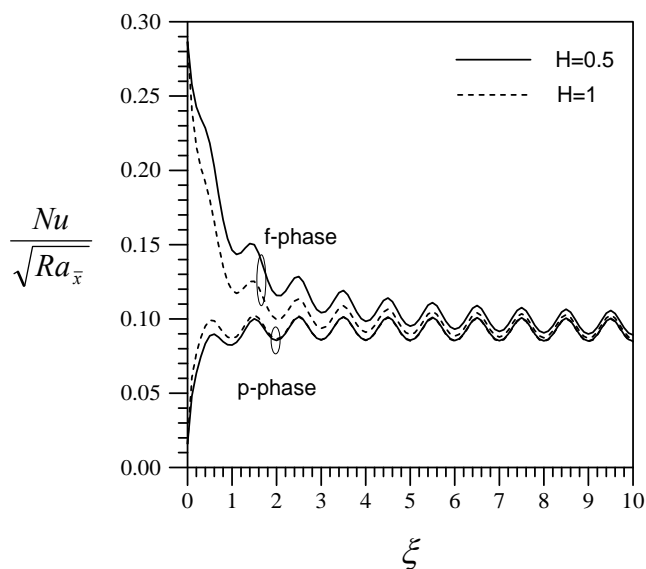


Fig. 7 The effect of the inter-phase heat transfer parameter on the local Nusselt numbers for the f-phase and the p-phase for $a = 0.2$, $Kr = 0.01$, $\beta = 1$, $\gamma = 0.1$, $\sigma_f = 0.01$, $\phi = 0.5$, $\varepsilon = 0.4$, and $\tau = 5/7$.

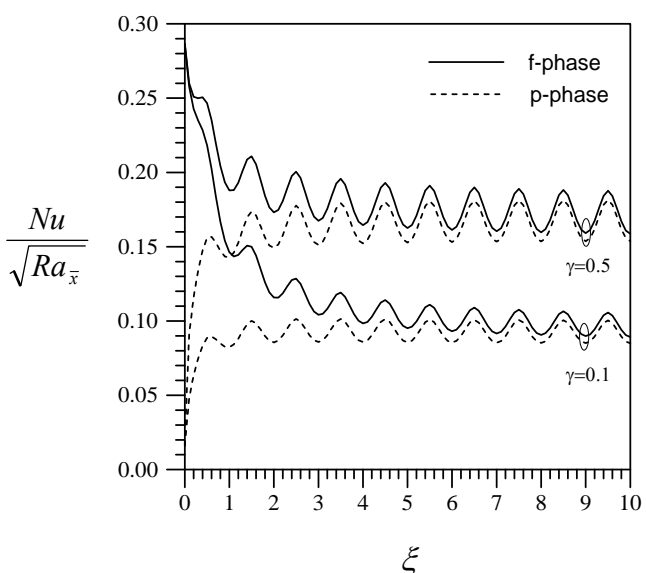


Fig. 8 The effect of the modified thermal conductivity ratio on the local Nusselt numbers for the f-phase and the p-phase for $a = 0.2$, $H = 0.5$, $Kr = 0.01$, $\beta = 1$, $\sigma_f = 0.01$, $\phi = 0.5$, $\varepsilon = 0.4$, and $\tau = 5/7$.

Fig. 7 shows the effect of the inter-phase heat transfer parameter H on the local Nusselt numbers for the f-phase and the p-phase. For a vertical wavy surface, decreasing the

inter-phase heat transfer parameter tends to increase the difference between local Nusselt numbers for the f-phase and the p-phase. In other words, lower values of the inter-phase heat transfer parameter leads to the state of thermal non-equilibrium between the p-phase and the f-phase of the bidisperse porous medium.

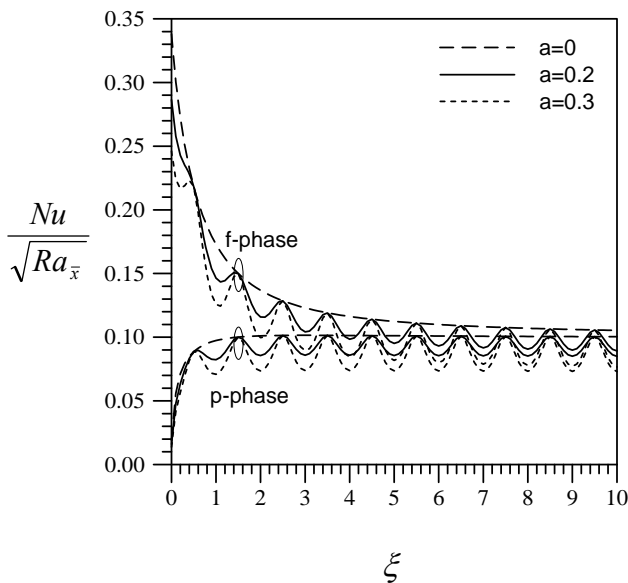


Fig. 9 The effect of the dimensionless amplitude on the local Nusselt numbers for the f-phase and the p-phase for $H = 0.5$, $Kr = 0.01$, $\beta = 1$, $\gamma = 0.1$, $\sigma_f = 0.01$, $\phi = 0.5$, $\varepsilon = 0.4$, and $\tau = 5/7$.

Fig. 8 shows the effect of the modified thermal conductivity ratio γ on the local Nusselt numbers for the f-phase and the p-phase. For a vertical wavy surface, increasing the modified thermal conductivity ratio γ tends to increase both the local Nusselt number for the f-phase and local Nusselt number for the p-phase. In other words, the heat transfer rate for the bidisperse porous medium can be effectively increased by increasing the modified thermal conductivity ratio.

Fig. 9 shows the effect of the dimensionless amplitude a on the local Nusselt number for the f-phase and the p-phase. As the dimensionless amplitude increases, both the fluctuations of the local Nusselt number for the f-phase and the p-phase with the streamwise coordinate become larger. Moreover, the values of the local Nusselt numbers for the f-phase higher than those for the p-phase.

IV. CONCLUSION

This work has studied the free convection about a vertical wavy surface in bidisperse porous media with constant wall temperature. This work uses both the two-velocity two-temperature model and the coordinate transformation to obtain the nonsimilar boundary layer differential equations. The cubic spline collocation method is used to solve the boundary layer equations. The effects of the inter-phase heat transfer parameter, the modified thermal conductivity ratio, and the permeability ratio on the free convection heat transfer characteristics have been studied. Results show an increase in the modified thermal

conductivity ratio or the permeability ratio tends to increase the free convection heat transfer rate of the vertical wavy surface in a bidisperse porous medium. Moreover, increasing the inter-phase heat transfer parameter tends to enhance the thermal non-equilibrium effect between the p-phase and the f-phase of the bidisperse porous medium. Increasing the dimensionless amplitude increases both the fluctuations of the local Nusselt number for the f-phase and the p-phase with the streamwise coordinate.

REFERENCES

- [1] D.A. Nield and A. V. Kuznetsov, "Forced Convection in Bi-disperse Porous Medium Channel: a Conjugate Problem," *International Journal of Heat and Mass Transfer*, vol.47, pp. 5375-5380, 2004.
- [2] D.A. Nield and A. V. Kuznetsov, "A Two-velocity Two-temperature Model for a Bi-disperse Porous Medium: Forced Convection in a Channel," *Transport in Porous Media*, vol.59, pp. 325-339, 2005.
- [3] D.A. Nield and A. V. Kuznetsov, "The Onset of Convection in a Bidisperse Porous Medium," *International Journal of Heat and Mass Transfer*, vol.49, pp. 3068-3074, 2006.
- [4] D. A. Nield and A. V. Kuznetsov, "The Effect of Combined Vertical and Horizontal Heterogeneity on the Onset of Convection in a Bidisperse Porous Medium," *International Journal of Heat and Mass Transfer*, vol.50, pp. 3329-3339, 2007.
- [5] D. A. Nield and A. V. Kuznetsov, "Natural Convection about a Vertical Plate Embedded in a Bidisperse Porous Medium," *International Journal of Heat and Mass Transfer*, vol.51, pp. 1658-1664, 2008.
- [6] D.A.S. Rees, D.A. Nield, and A. V. Kuznetsov, "Vertical Free Convective Boundary-layer Flow in a Bidisperse Porous Medium," *ASME Journal of Heat Transfer*, vol.130, pp. 092601.1-092601.9, 2008.
- [7] B. Straughan, "On the Nield-Kuznetsiv Theory for Convection in Bidisperse Porous Media," *Transport in Porous Media*, vol.77, pp. 159-168, 2009.
- [8] Kumari, M. and Pop, I., "Mixed Convection Boundary Layer Flow past a Horizontal Circular Cylinder Embedded in a Bidisperse Porous Medium," *Transport in Porous Media*, vol.77, pp.287-303, 2009.
- [9] T. Grosan, I. Pop, and D. B. Ingham, "Free Convection in a Square Cavity Filled with a Bidisperse Porous Medium," *International Journal of Thermal Sciences*, vol.48, pp.1876-1883, 2009.
- [10] A. Narasimhan and B.V.K. Reddy, "Natural Convection Inside a Bidisperse Porous Medium Enclosure," *ASME Journal of Heat Transfer*, Vol.132, pp. 012502.1-012502.9, 2010.
- [11] A. Narasimhan and B.V.K. Reddy, "Resonance of Natural Convection inside a Bidisperse Porous Medium Enclosure," *ASME Journal of Heat Transfer*, vol.133, pp. 042601.1-042601.9, 2011.
- [12] D. A. Nield and A. V. Kuznetsov, "Forced Convection in a Channel Partly Occupied in a Bidisperse Porous Medium: Symmetric Case," *ASME Journal of Heat Transfer*, vol.133, pp. 072601.1-072601.9, 2011.
- [13] K. A. Yih, "Coupled Heat and Mass Transfer by Free Convection over a Truncated Cone in Porous Media: VWT/VWC or VHF/VMF," *Acta Mechanica*, vol.137, pp.83-97, 1999.
- [14] P. Wang and R. Kahawita, "Numerical Integration of a Partial Differential Equations Using Cubic Spline," *International Journal of Computers and Mathematics*, vol.13, pp. 271-286, 1983.
- [15] P. Cheng, W.J. Minkowycz, "Free Convection about a Vertical Plate Embedded in a Porous Medium with Application to Heat Transfer from a Dyke," *Journal of Geophysics Research*, vol. 82, pp. 2040-2044, 1977.
- [16] D.A.S. Rees, I. Pop, "Vertical Free Convective Boundary-layer Flow in a Porous Medium Using a Thermal Nonequilibrium Model," *Journal of Porous Media*, vol. 3, pp. 31-44, 2000.